J|A|C|S
ARTICLES
Published on Web 09/08/2006

DFT Studies on the Mechanism of Allylative Dearomatization Catalyzed by Palladium

Alireza Ariafard[†,‡] and Zhenyang Lin*[,‡]

Contribution from the Department of Chemistry, Faculty of Science, Central Tehran Branch, Islamic Azad University, Felestin Square, Tehran, Iran, and Department of Chemistry and Open Laboratory of Chirotechnology of the Institute of Molecular Technology for Drug Discovery and Synthesis, The Hong Kong University of Science and Technology, Clear Water Bay, Kowloon, Hong Kong

Received June 5, 2006; E-mail: chzlin@ust.hk

Abstract: The reaction mechanism of the Pd-catalyzed benzyl/allyl coupling of benzyl chloride with allyltributylstannan, resulting in the dearomatization of the benzyl group, was studied using density functional theory calculations at the B3LYP level. The calculations indicate that the intermediate (η^3-benzyl)(η^1-allyl)-Pd(PH_3) is responsible for the formation of the kinetically favored dearomatic product. Reductive elimination of the dearomatic product from the intermediate occurs by coupling the C-3 terminus of the η^1-allyl ligand and the *para*-carbon of the η^3-benzyl ligand in (η^3-benzyl)(η^1-allyl)Pd(PH_3). For comparison, various C−C coupling reaction pathways have also been examined.

Introduction

The special stability due to the delocalization of π bonds makes dearomatization of arenes very difficult.[1] Recently, Yamamoto and co-workers reported dearomatization reactions of benzyl chlorides with allyltributylstannane catalyzed by Pd-(0) complexes (Scheme 1).[2] The reactions are interesting and unusual because palladium-catalyzed coupling reactions of organostannanes (e.g., $RSnBu_3$) with organic halides (R′X), known as Stille coupling,[3−5] usually give the products R−R′ that are derived by coupling the R and R′ groups directly without changing their individual configurations.[6,7] For example, a very closely related Stille coupling of benzyl bromide with vinyltributylstannane gives allylbenzene (Scheme 2).[8]

Scheme 1

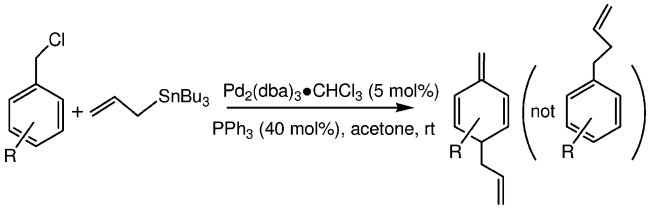

Scheme 2

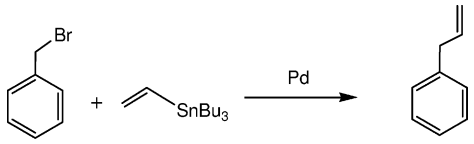

To account for the dearomatization reactions, Yamamoto and co-workers[2] proposed a reaction mechanism, shown in Scheme 3, which involves oxidative addition, transmetalation, and reductive elimination as found in the Stille coupling catalytic cycle. The key feature of the proposed reaction mechanism is the formation of η^3-benzyl intermediates from which rearrangement of the η^3-benzyl ligand from an η^3-*exo*-benzyl to an η^3-

† Islamic Azad University.
‡ The Hong Kong University of Science and Technology.

(1) (a) Barner, B. A.; Meyers, A. I. *J. Am. Chem. Soc.* **1984**, *106*, 1865. (b) Maruoka, K.; Ito, M.; Yamamoto, H. *J. Am. Chem. Soc.* **1995**, *117*, 9091. (c) Berger, R.; Ziller, J. W.; Vranken, D. L. V. *J. Am. Chem. Soc.* **1998**, *120*, 841. (d) Schultz, A. G. *Chem. Commun.* **1999**, 1263. (e) Pape, A. R.; Kaliappan, K. P.; Kündig, E. P. *Chem Rev.* **2000**, *100*, 2917. (f) Chordia, M. D.; Harman, W. D. *J. Am. Chem. Soc.* **2000**, *122*, 2725. (g) Graham, P. M.; Meiere, S. H.; Sabat, M.; Harman, W. D. *Organometallics* **2003**, *22*, 4364. (h) Ding, F.; Valahovic, M. T.; Keane, J. M.; Anstey, M. R.; Sabat, M.; Trindle, C. O.; Harman, W. D. *J. Org. Chem.* **2004**, *69*, 2257. (i) Fernandez, I.; Gonzalez, J.; Lopez-Ortiz, F. *J. Am. Chem. Soc.* **2004**, *126*, 12551. (j) Keane, J. M.; Harman, W. D. *Organometallics* **2005**, *24*, 1786. (k) Delafuente, D. A.; Myers, W. H.; Sabat, M.; Harman, W. D. *Organometallics* **2005**, *24*, 1885. (l) Zhu, J.; Grigoriadis, N. P.; Lee, J. P.; Porco, J. A., Jr. *J. Am. Chem. Soc.* **2005**, *127*, 9342. (m) Jantunen, K. C.; Scott, B. L.; Hay, P. J.; Gordon, J. C.; Kiplinger, J. L. *J. Am. Chem. Soc.* **2006**, *128*, 6322. (n) Zhou, L.; Wu, L.-Z.; Zhang, L.-P.; Tung, C.-H. *Organometallics* **2006**, *25*, 1707. (o) Monje, P.; Grana, P.; Paleo, M. R.; Sardina, F. *J. Org. Lett.* **2006**, *8*, 954. (p) Pigge, F. C.; Coniglio, J. J.; Dalvi, R. *J. Am. Chem. Soc.* **2006**, *128*, 3498.
(2) Bao, M.; Nakamura, H.; Yamamoto; Y. *J. Am. Chem. Soc.* **2001**, *123*, 759.
(3) (a) Milstein, D.; Stille, J. K. *J. Am. Chem. Soc.* **1978**, *100*, 363. (b) Stille, J. K. *Angew. Chem., Int. Ed. Engl.* **1986**, *25*, 508.
(4) (a) Farina, V. In *Comprehensive Organometallic Chemistry II*; Abel, E. W., Stone, F. G. A., Wilkinson, G., Eds.; Pergamon: Oxford, U.K., 1995; Vol. 12. (b) Mitchell, T. N. In *Metal-catalyzed cross-coupling Reactions*; Diederich, F., Stang, P. J., Eds.; Wiley-VCH: New York, 1998. (c) Kosugi, M.; Fugami, K. In *Handbook of Organopalladium chemistry for Organic Synthesis*; Negishi, E., Ed.; Wiley: New York, 2002. (d) Tsuji, J. *Palladium Reagents and Catalysts*; Wiley: Chichester, U.K., 2004.
(5) (a) Espinet, P.; Echavarren, A. M. *Angew. Chem., Int. Ed.* **2004**, *43*, 4704. (b) Nicolaou, K. C.; Bulger, P. G.; Sarlah, D. *Angew. Chem., Int. Ed.* **2005**, *44*, 4442.
(6) (a) Farina, V.; Roth, G. P. *Adv. Met.-Org. Chem.* **1996**, *5*, 1. (b) Farina, V. *Pure Appl. Chem.* **1996**, *68*, 73. (c) Casado, A. L.; Espinet, P. *J. Am. Chem. Soc.* **1998**, *120*, 8978. (d) Casado, A. L.; Espinet, P.; Gallego, A. M. *J. Am. Chem. Soc.* **2000**, *122*, 11771.
(7) (a) Crawforth, C. M.; Fairlamb, I. J. S.; Taylor, R. J. K. *Tetrahedron Lett.* **2004**, *45*, 461. (b) Serrano, J. L.; Fairlamb, I. J. S.; Sánchez, G.; García, L.; Pérez, J.; Vives, J.; López, G.; Crawforth, V.; Taylor, R. J. K. *Eur. J. Inorg. Chem.* **2004**, 2706. (c) Crawforth, C. M.; Burling, S.; Fairlamb, I. J. S.; Kapdi, A. R.; Taylor, R. J. K.; Whitwood, A. C. *Tetrahedron* **2005**, *61*, 9736.
(8) Milstein, D.; Stille, J. K. *J. Am. Chem. Soc.* **1979**, *101*, 4992.

10.1021/ja063944i CCC: $33.50

Scheme 3

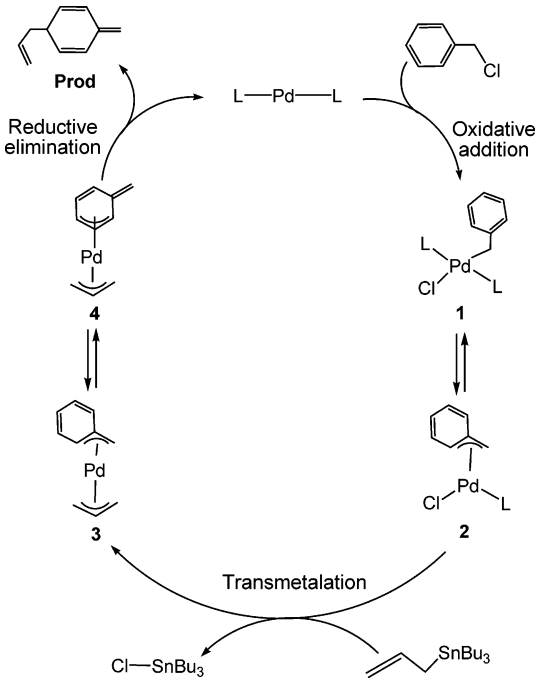

endo-benzyl coordination mode occurs, giving the possibility to reductively eliminate the dearomatic products.[2,4d,5a,9]

Many interesting questions arise when we compare the reactions shown in Schemes 1 and 2, both involving benzyl halides. If rearrangement of the η^3-benzyl ligand from an η^3-*exo*-benzyl to an η^3-*endo*-benzyl coordination mode could occur, why do not we observe dearomatic products from the coupling reaction of benzyl bromide with vinyltributylstannane? Does the η^3-allyl ligand, originally from the allyltributylstannane reagent, promote the η^3-*exo*-benzyl to η^3-*endo*-benzyl rearrangement? If yes, how does the η^3-allyl ligand (in comparison with the vinyl ligand) promote the rearrangement? If not, is there a new coupling pathway to account for the experimental observations? The objectives of this work are to address these important questions with the aid of DFT calculations at the B3LYP level by examining the structural and energetic aspects of various possible reaction pathways. We hope that the findings presented in this article help scientists in designing new catalysts for dearomatization of naturally abundant aromatic compounds.

Computational Details

Molecular geometries of the model complexes were optimized without constraints at the Becke3LYP (B3LYP)[10] level of density functional theory. The effective core potentials of Hay and Wadt with double-ζ valance basis sets (LanL2DZ)[11] were used for Pd and P. The 6-31G[12] basis set was chosen to describe C and H. Polarization functions were also added for C ($\xi_d = 0.6$) and P ($\xi_d = 0.34$).[13] Frequencies were analytically computed at the same level of theory to confirm whether the structures are minima or transition states, as appropriate.

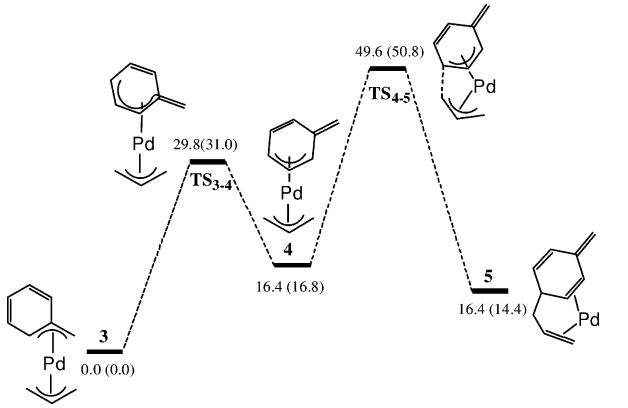

Figure 1. Energy profile for the **3** → **4** rearrangement and the reductive elimination from **4**. The relative free energies and electronic energies (in parentheses) are given in kcal/mol.

Scheme 4

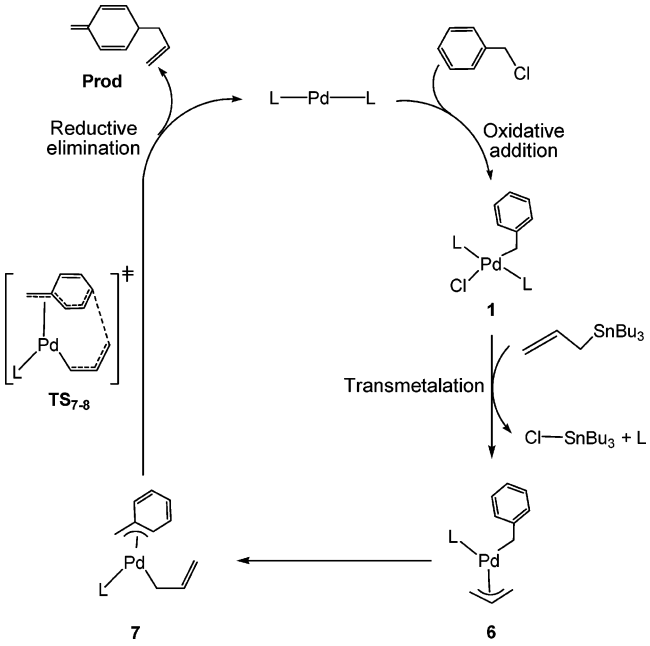

Calculations of intrinsic reaction coordinates (IRC)[14] were also performed on transition states to confirm that such structures are indeed connecting two minima. To estimate the degree of aromaticity of the benzyl ligands, nucleus-independent chemical shift (NICS)[15] calculations were performed using the GIAO[16] method and at the B3LYP level. For the NICS calculations, we replaced the 6-31G basis set mentioned above by 6-311G(d,p) basis set. All calculations were performed with the Gaussian 03[17] software package.

Results and Discussion

Reaction Mechanisms. Let us first discuss the mechanism proposed by Yamamoto and co-workers. As mentioned in the Introduction, the key feature of the Yamamoto mechanism is the rearrangement of the η^3-benzyl ligand from an η^3-*exo*-benzyl coordination mode in **3** to an η^3-*endo*-benzyl coordination mode in **4**. Therefore, we calculated the **3** → **4** rearrangement step

(9) Söderberg, B. C. G. *Coord. Chem. Rev.* **2003**, *247*, 79.
(10) (a) Lee, C.; Yang, W.; Parr, G. *Phys. Rev.* **1988**, *B37*, 785. (b) Miehlich, B.; Savin, A.; Stoll, H.; Preuss, H. *Chem. Phys. Lett.* **1989**, *157*, 200. (c) Becke, A. D. *J. Chem. Phys.* **1993**, *98*, 5648.
(11) (a) Wadt, W. R.; Hay, P. J. *J. Chem. Phys.* **1985**, *82*, 284. (b) Hay, P. J.; Wadt, W. R. *J. Chem. Phys.* **1985**, *82*, 299.
(12) Hariharan, P. C.; Pople, J. A. *Theor. Chim. Acta* **1973**, *28*, 213.
(13) Huzinaga, S. *Gaussian Basis Sets for Molecular Calculations*; Elsevier Science Pub. Co.: Amsterdam, 1984.
(14) (a) Fukui, K. *J. Phys. Chem.* **1970**, *74*, 4161. (b) Fukui, K. *Acc. Chem. Res.* **1981**, *14*, 363.
(15) Schleyer, P. v. R.; Maerker, C.; Dransfeld, A.; Jiao, H.; Hommes, N. J. R. v. E.*J. Am. Chem. Soc.* **1996**, *118*, 6317.
(16) Wolinski, K.; Hinton, J. F.; Pulay, P. *J. Am. Chem. Soc.* **1990**, *112*, 8251.
(17) Frisch, M. J.; et al. *Gaussian 03*, revision B05; Gaussian, Inc.: Pittsburgh, PA, 2003.

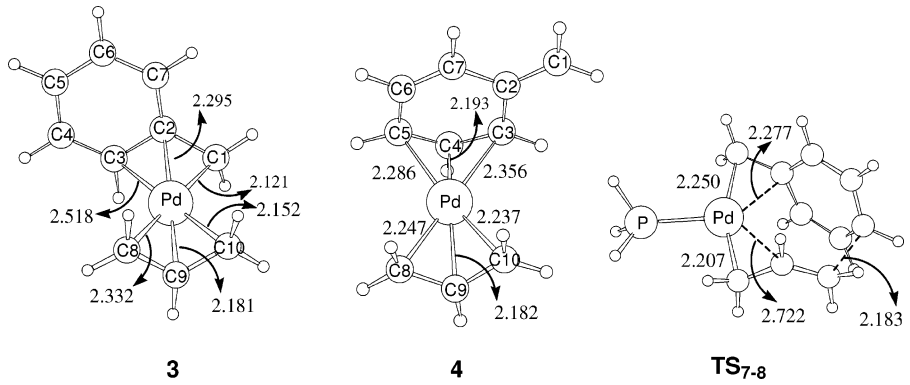

Figure 2. Optimized structures with selected bond lengths (Å) for **3**, **4**, and $\mathbf{TS}_{7-8}$.

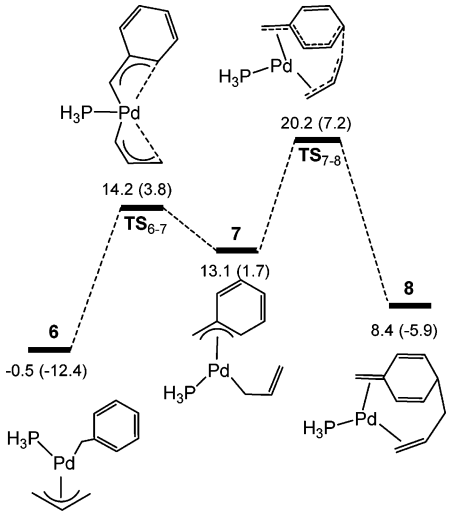

Figure 3. Energy profile for the **6** → **7** isomerization followed by the reductive elimination. The relative free energies and electronic energies (in parentheses) are given in kcal/mol.

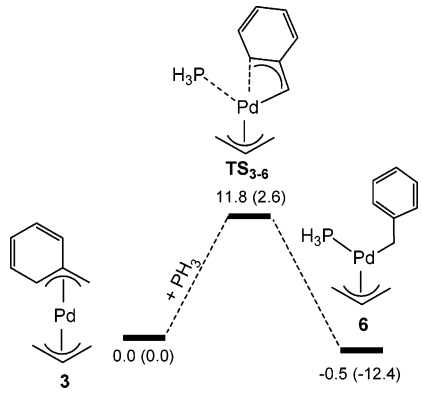

Figure 4. Energetics for the **3** → **6** conversion. The relative free energies and electronic energies (in parentheses) are given in kcal/mol.

and the reductive elimination step from **4**. The calculated energy profile for the two steps is shown in Figure 1. From Figure 1, we see that the rearrangement from **3** to **4** is endothermic (ΔG_{298} = 16.4 kcal/mol) and requires an activation energy of 29.8 kcal/mol. The reductive elimination of the dearomatic product **Prod** from **4** needs an even higher activation energy (33.2 kcal/mol). The overall barrier from **3** to **5** is 49.6 kcal/mol. Clearly, the overall barrier is too high for the proposed mechanism to be energetically feasible.

The proposed intermediate **4** is noticeably unstable in comparison with **3**. We believe that it is the poorer aromaticity

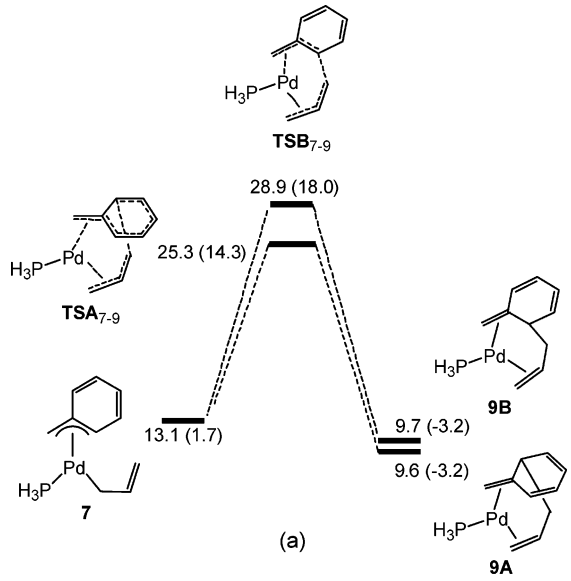

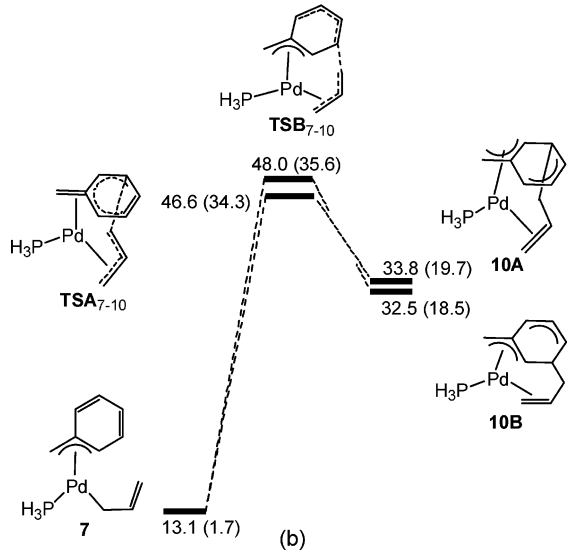

Figure 5. Energy profiles for four other possible reductive elimination pathways from **7**. The relative free energies and electronic energies (in parentheses) are given in kcal/mol.

of the η^3-*endo*-benzyl ligand in **4** versus the η^3-*exo*-benzyl ligand in **3** that makes **4** unstable because comparison of the structural parameters in the Pd−η^3-benzyl structural moieties between **3** and **4** (Figure 2) does not give us a clue behind the energy difference. Nucleus-independent chemical shift (NICS, a mea-

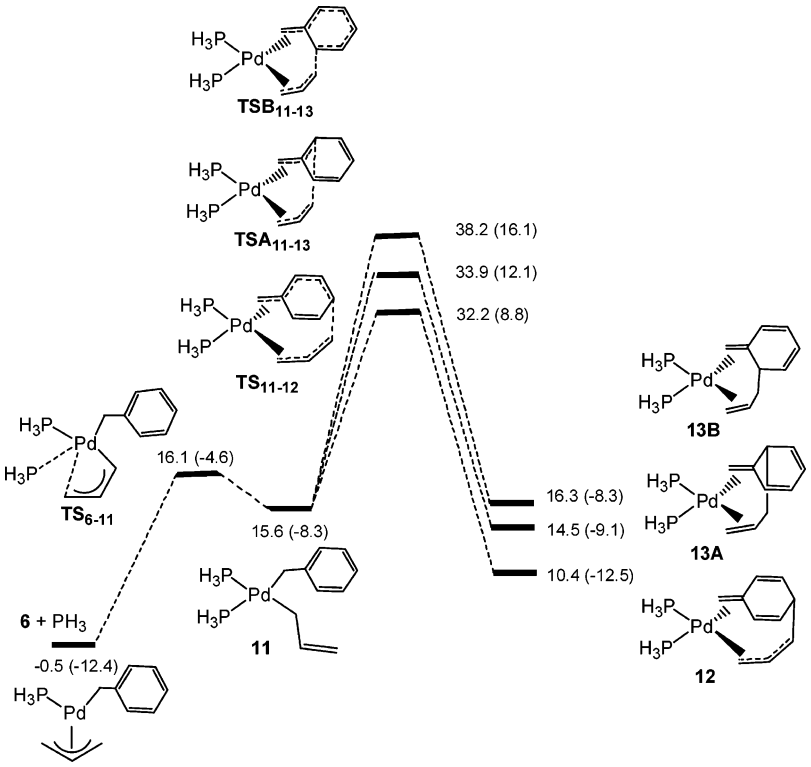

Figure 6. Energy profiles for the formation of **11** from **6** followed by reductive elimination. The relative free energies and electronic energies (in parentheses) are given in kcal/mol.

sure of aromaticity) calculations were performed to support the claim above. NICS(0) values were calculated at the center of the phenyl ring in the benzyl ligand, found by averaging the coordinates of the six carbon atoms forming the ring. NICS(1) values were calculated at a point 1.0 Å away from the center of the pheny ring, in a direction perpendicular to the plane of the ring. The NICS(1) [NICS(0)] values of −8.1 [−5.7] and −1.8 [−1.4] were calculated for **3** and **4**, respectively, indicating that the phenyl ring in the benzyl ligand of **3** has higher degree of aromaticity than that of **4**.

From the energy profile shown in Figure 1, it is clear that the mechanism proposed by Yamamoto is energetically unfeasible. Thus, a new mechanism other than the proposed mechanism should be operative. Scheme 4 shows the new mechanism we proposed. We assume that transmetalation occurs between **1** and allyltributylstannane to give **6**. **6** isomerizes to **7** followed by a reductive elimination to give the product. The important step of this newly proposed mechanism is the reductive elimination directly from **7** via $\mathbf{TS}_{7-8}$ (Figure 2) in which a direct coupling between the C-3 terminus of the η^1-allyl ligand and the *para*-carbon of the η^3-benzyl ligand is hypothesized. The hypothesis is formulated on the basis of a recent theoretical finding that the intramolecular allyl−allyl coupling prefers a pathway via the formation of the C−C bond between the C-3 termini of the allyl ligands in a bis(η^1-allyl)metal complex.[18a] (η^1-Allyl)palladium(II) complexes have also been proposed as feasible intermediates in Pd-catalyzed reactions in a recent theoretical study.[18b]

Our calculations provide firm support to the hypothesis. Figure 3 shows the energy profile for the **6** → **7** isomerization followed by a reductive elimination. **8** is a precursor complex containing the product molecule (**Prod**) as a ligand. The activation free energy required for the isomerization is calculated to be 14.7 kcal/mol. The isomerization is found to be endothermic, indicating that (η^1-benzyl)(η^3-allyl)PdL (**6**) is more stable than (η^3-benzyl)(η^1-allyl)PdL (**7**). The instability of (η^3-benzyl)(η^1-allyl)PdL (**7**) reflects a weaker metal coordination of η^3-benzyl versus η^3-allyl. The reductive elimination from **7** by coupling the C-3 terminus of the η^1-allyl ligand and the *para*-carbon of the η^3-benzyl ligand via $\mathbf{TS}_{7-8}$ has a barrier of only 7.1 kcal/mol. The overall barrier from **7** to **8** (20.7 kcal/mol) is only moderate, demonstrating the feasibility of the newly proposed mechanism in Scheme 4.

On the basis of Scheme 4, one may think that there is a possible pathway for **6** to loss a phosphine ligand[19] to form **3**. Figure 4 shows that **6** can indeed be in equilibrium with **3**. The barrier for the interconversion is relatively small. **6** is slightly more stable than **3** in terms of their Gibbs free energies. Clearly, **3** is not particularly stable, likely due to the weak Pd−η^3-benzyl bonding interaction. The Pd−C2 and Pd−C3 distances in the Pd−η^3-benzyl structural moiety **3** are remarkably long (Figure 2).

Pathways Leading to Other Dearomatic Products. Starting from **7**, we can also have four other possible reductive elimination pathways, apart from the one discussed above. These pathways correspond to coupling of the C-3 terminus of the η^1-allyl with the *ortho*- and *meta*-carbons of the η^3-benzyl ligand, leading to the formation of the dearomatic products **Prod_1** and **Prod_2**, respectively. Figure 5 shows the energy profiles calculated for the four possible reductive elimination pathways. The pathways giving **Prod_1** occur via $\mathbf{TSA}_{7-9}$ and

(18) (a) Méndez, M.; Cuerva, J. M.; Gómez-Bengoa, E.; Cárdenas, D. J.; Echavarren, A. M. *Chem.—Eur. J.* **2002**, *8*, 3620. (b) García-Iglesias, M.; Buñuel, E.; Cárdenas, D. J. *Organometallics* **2006**, *25*, 3611.

(19) Solin, N.; Szabó, K. J. *Organometallics* **2001**, *20*, 5464.

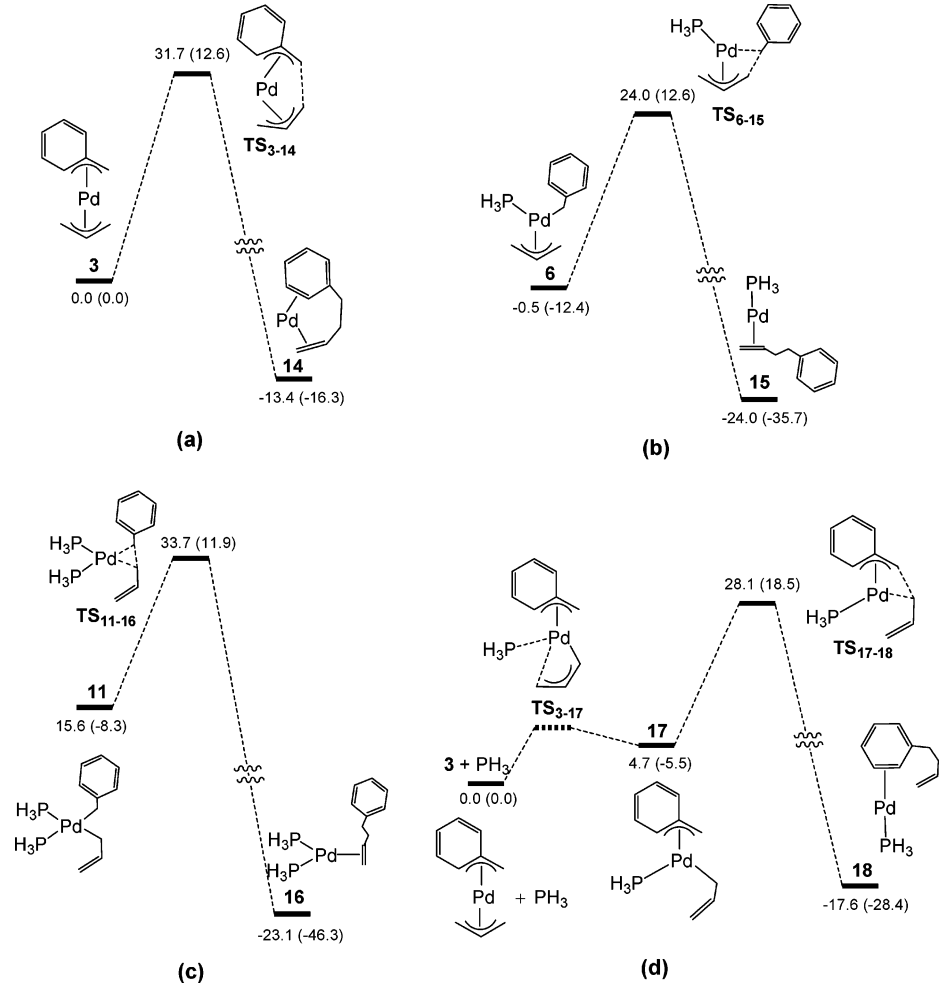

Figure 7. Energy profiles for direct coupling from intermediates **3**, **6**, **11**, and **17** (an orientational isomer of **7**) to give the corresponding precursor complexes **14**, **15**, **16**, and **18**, respectively, that have **Prod_3** as a ligand. The relative free energies and electronic energies (in parentheses) are given in kcal/mol.

TSB$_{7-9}$ while those giving **Prod_2** occur via **TSA**$_{7-10}$ and **TSB**$_{7-10}$. The transition states, especially **TSA**$_{7-10}$ and **TSB**$_{7-10}$, are significantly higher in energy than **TS**$_{7-8}$, supporting the conclusion that the most favorable pathway for the reductive elimination is the coupling of the C-3 terminus of the η^1-allyl ligand with the *para*-carbon of the η^3-benzyl ligand. These results are consistent with the experimental observation that **Prod**, instead of **Prod_1** or **Prod_2**, is the only product isolated. The relative energies of the transition states **TSA**$_{7-9}$, **TSB**$_{7-9}$, **TSA**$_{7-10}$, and **TSB**$_{7-10}$ correlate well with those of **9A**, **9B**, **10A**, and **10B**, respectively. **Prod** is calculated to be about 3.9 and 57.9 kcal/mol more stable than **Prod_1** and **Prod_2**, respectively. All these results indicate that the relative stability of the dearomatic products **Prod_1** and **Prod_2** plays a certain role in the relative stability of the transition states (**TS**$_{7-8}$, **TSA**$_{7-9}$, **TSB**$_{7-9}$, **TSA**$_{7-10}$, and **TSB**$_{7-10}$) as well as the reductive elimination products (**8**, **9A**, **9B**, **10A**, and **10B**).

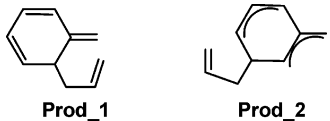

Another possible intermediate from which the dearomatic products **Prod**, **Prod_1**, and **Prod_2** can be obtained is the (η^1-allyl)palladium complex **11** having two phosphine ligands (Figure 6). **Prod_2** is too unstable, and therefore, we will not discuss its formation here. **11** is formed by coordination of a PH_3 ligand and rearrangement of the η^3-allyl coordination mode to an η^1-allyl mode in **6** (Figure 6). The **6** → **11** conversion proceeds via the transition state **TS**$_{6-11}$ and is an endothermic process (ΔG_{298} = 16.1 kcal/mol) due to the low stability of the η^1-allyl structure. Among the three reductive elimination pathways shown in Figure 6, the pathway corresponding to a direct coupling between the C-3 terminus of the η^1-allyl ligand and the *para*-carbon of the η^1-benzyl ligand was calculated to be most favored, a result consistent with the finding we discussed above for the reductive elimination from **7**. Again, the overall barriers for the reductive elimination going through **11** to give precursor complexes of **Prod** and **Prod_1** are high. Therefore, the corresponding pathways cannot be responsible for the formation of the dearomatic products.

Pathways Leading to the Usually Expected Stille Coupling Product. As mentioned in the Introduction, palladium-catalyzed coupling reactions of organostannanes (e.g., $RSnBu_3$) with organic halides (R′X) (Stille coupling) usually give the products R−R′ that are derived by coupling the R and R′ groups directly without changing their individual configurations. We now come to examine the reaction barriers for pathways directly coupling

Scheme 5

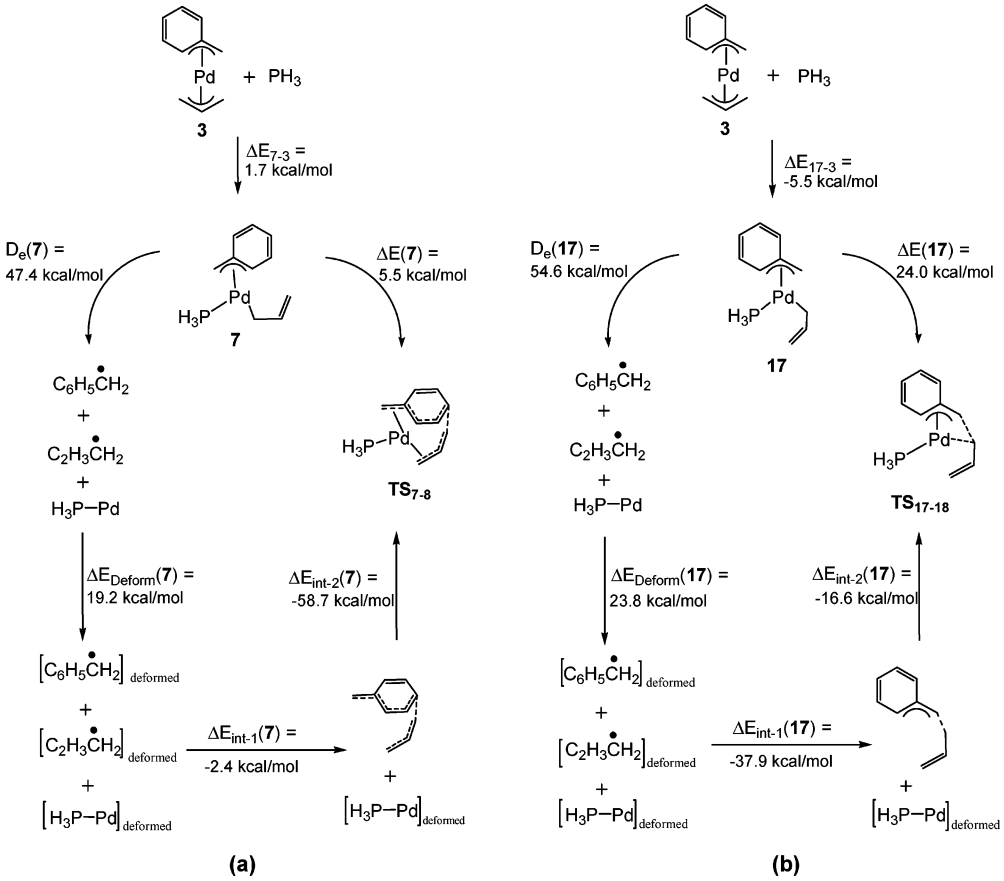

the allyl and benzyl groups and to see why the usually expected coupling product **Prod_3** was not observed in the reaction of benzyl chloride with allyltributylstannane.

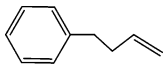

Prod_3

We considered intermediates **3**, **6**, **11**, and **17** (an orientational isomer of **7**) for direct coupling to give the corresponding precursor complexes **14**, **15**, **16**, and **18**, respectively, having **Prod_3** as a ligand. Figure 7 shows the energy profiles. The relative energies for the direct coupling transition states $\mathbf{TS}_{3-14}$, $\mathbf{TS}_{6-15}$, $\mathbf{TS}_{11-15}$, and $\mathbf{TS}_{17-18}$ are calculated to be 31.7, 24.0, 33.7, and 28.1 kcal/mol, respectively. Consistent with the experimental observation, all the direct coupling transition states are much higher in energy than that calculated for the most favorable transition state $\mathbf{TS}_{7-8}$ (20.2 kcal/mol, Figure 3) leading to the formation of the experimentally observed coupling product **Prod**. The precursor complexes **14**, **15**, **16**, and **18** having the usually expected coupling product **Prod_3** as a ligand are relatively much more stable than the precursor complex **8** having the dearomatic product **Prod** as a ligand. Clearly, the relative stability of these precursor complexes is closely related to the relative stability of the coupling products that act as ligands. **Prod_3** is calculated to be more stable than **Prod** by 31.0 kcal/mol. Thus, the reductive elimination via the transition state $\mathbf{TS}_{7-8}$ is kinetically, not thermodynamically, favored over the reductive elimination via the transition states $\mathbf{TS}_{3-14}$, $\mathbf{TS}_{6-15}$, $\mathbf{TS}_{11-16}$, and $\mathbf{TS}_{17-18}$. We failed to locate the transition state $\mathbf{TS}_{3-17}$ (Figure 7d) giving the orientational isomer **17**, due to the fact that the potential energy surface connecting **3** and **17** is flat.

Dearomatization versus Stille Coupling. To understand why the transition state $\mathbf{TS}_{7-8}$ is much more stable when compared with those related to the direct coupling, we carried out an energy decomposition analysis[20] (Scheme 5) on the reaction barriers of **7** → **8** and **17** → **18**. In Scheme 5, we can see that **7** is less stable than its orientational isomer **17**. We noted that the C1 atom of the benzyl ligand has a stronger interaction with the metal center than the C3 atom, evidenced by the shorter Pd−C1 bond distances in both **7** and **17** (Figure 8). The structural arrangement in **7** is expected to be less favorable considering the trans influence properties of both the η^1-allyl and η^3-benzyl ligands.

In Scheme 5, D_e represents the energy required to dissociate fragment (η^1-allyl)(η^3-benzyl)Pd(PH_3) (**17** or **7**) into three fragments: benzyl radical; allyl radical; $Pd(PH_3)_2$. ΔE_{Deform} refers to the energy needed to deform the three fragments to the geometries they have in the transition states. The interaction energy between the deformed benzyl and allyl fragments in the transition state is represented by $\Delta E_{\text{int}-1}$, and the interaction energy between the combined deformed organic fragments and the deformed $Pd(PH_3)_2$ metal fragment, by $\Delta E_{\text{int}-2}$. A comparison between parts a and b of Scheme 5 shows that the significant difference between the energy barriers of **7** → **8** via $\mathbf{TS}_{7-8}$ and **17** → **18** via $\mathbf{TS}_{17-18}$ is related to both the difference between

(20) (a) Ziegler, T.; Rauk, A. *Theor. Chim. Acta* **1977**, *46*, 1. (b) Bickelhaupt, F. M. *J. Comput. Chem.* **1999**, *20*, 114.

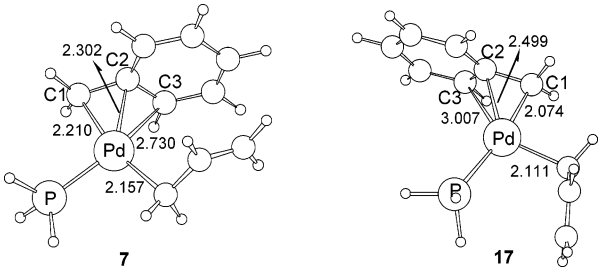

Figure 8. Optimized structures with selected bond lengths (Å) for **7** and **17**.

ΔE_{int-1}(**7**) and ΔE_{int-1}(**17**) and the difference between ΔE_{int-2}(**7**) and ΔE_{int-2}(**17**). ΔE_{int-1}(**7**) is very small (−2.4 kcal/mol) because the benzyl aromaticity is being broken while ΔE_{int-1}(**17**) is large (−37.9 kcal/mol) because a new C−C bond is being formed without breaking the benzyl aromaticity. The difference between ΔE_{int-1}(**7**) and ΔE_{int-1}(**17**) is 35.5 kcal/mol. In contrast, ΔE_{int-2}(**7**) (−58.7 kcal/mol) is much more negative than ΔE_{int-2}(**17**) (−16.6 kcal/mol), suggesting that the complexation energy between $Pd(PH_3)_2$ and the benzyl---allyl organic moiety in $\mathbf{TS}_{7-8}$ is very large. The difference between ΔE_{int-2}(**7**) and ΔE_{int-2}(**17**) is −41.9 kcal/mol. Clearly, it is mainly the large interaction energy ΔE_{int-2}(**7**) that gives the smaller barrier calculated for the **7** → **8** step when compared to the **17** → **18** step. The energy decomposition anaylsis given above indicates that the benzyl and allyl ligands maintain strong coordination with the Pd metal center in the transition state structure $\mathbf{TS}_{7-8}$. However, the benzyl and allyl ligands do not effectively bind to the Pd metal center in the transition state structure $\mathbf{TS}_{17-18}$. In other words, the reductive elimination via $\mathbf{TS}_{7-8}$ requires a minimum disruption in the metal−ligand bonding on going from **7** to $\mathbf{TS}_{7-8}$ while the elimination via $\mathbf{TS}_{17-18}$ requires a drastic change in the metal−ligand bonding on going from **17** to $\mathbf{TS}_{17-18}$.

Brief Comments on the Use of PH_3 as a Model Phosphine Ligand. In the calculations, we used PH_3 as a model for PPh_3. To study the steric effect missed from the small model calculations, we performed two-layer ONIOM (B3LYP/BSI:HF/Lanl2MB)[21] calculations with the real PPh_3 ligand for the **6** → $\mathbf{TS}_{7-8}$ and **6** → $\mathbf{TS}_{6-15}$ steps. In the ONIOM calculations, the phenyl groups on the phosphine ligand were treated as the second layer while the rest were treated as the first layer. BSI represents the basis set described in the Computational Details section. The **6** → $\mathbf{TS}_{7-8}$ step leads to the dearomatization product, while the **6** → $\mathbf{TS}_{6-15}$ step is the lowest pathway giving the Stille coupling product. The ONIOM calculation results show that the steric bulkiness of the PPh_3 ligand does not affect the barriers. In the PH_3 model calculations, the barriers in terms of electronic energies from **6** to $\mathbf{TS}_{7-8}$ and from **6** to $\mathbf{TS}_{6-15}$ are calculated to be 19.6 and 25.0 kcal/mol, respectively (see Figures 3 and 7b). In the PPh_3 calculations, the barriers from **6** to $\mathbf{TS}_{7-8}$ and from **6** to $\mathbf{TS}_{6-15}$ are calculated to be 18.9 and 25.1 kcal/mol, respectively. The geometry around the metal center in each of the structures calculated also does not change much (see the Supporting Information for more details). The results are understandable because of the low coordination number around the Pd metal center in the species involved.

(21) For references of the ONIOM method, see the following: (a) Dapprich, S.; Komáromi, I.; Byun, K. S.; Morokuma, K.; Frisch, M. J. *J. Mol. Struct. (THEOCHEM)* **1999**, *462*, 1. (b) Vreven, T.; Morokuma, K. *J. Comput. Chem.* **2000**, *21*, 1419. For a similar two-layer ONIOM calculation, see the following: (c) Ananikov, V. P.; Szilagyi, R.; Morokuma, K.; Musaev, D. G. *Organometallics* **2005**, *24*, 1938.

Summary

The dearomatization reactions of benzyl chlorides with allyltributylstannane catalyzed by Pd(0) complexes discovered by Yamamoto and co-workers have been theoretically studied using density functional theory calculations. On the basis of the DFT calculations, we found that the dearomatization reaction mechanism involves isomerization of (η^1-benzyl)(η^3-allyl)PdL (L = phosphine), which is formed by transmetalation between $L_2Pd(Ar)(Cl)$ and allyltributylstannane, to the intermediate (η^3-benzyl)(η^1-allyl)PdL, followed by reductive elimination through coupling of the C-3 terminus of the η^1-allyl ligand with the *para*-carbon of the η^3-benzyl ligand.

Reductive elimination starting from the intermediate (η^3-benzyl)(η^1-allyl)PdL through coupling of the C-3 terminus of the η^1-allyl with the *ortho*- or one of the *meta*-carbons of the η^3-benzyl ligand, which would give different dearomatic products, was also studied. These couplings were found to be both thermodynamically and kinetically less favored than the coupling between the C-3 terminus of the η^1-allyl ligand and the *para*-carbon of the η^3-benzyl ligand. Direct coupling between the benzyl and allyl groups, which gives the Stille coupling product, was also found to be kinetically less favorable.

Through an energy decomposition analysis, we found that reductive elimination from the intermediate (η^3-benzyl)(η^1-allyl)PdL through coupling of the C-3 terminus of the η^1-allyl ligand with the *para*-carbon of the η^3-benzyl ligand, which gives the dearomatic product, allows both the benzyl and allyl ligands to maintain strong coordination with the Pd metal center in the transition state structure, minimizing the disruption in the metal−ligand bonding on going from the intermediate to the transition state and making the dearomatization reactions kinetically favorable. Contrarily, the direct reductive elimination, which gives the Stille coupling product, requires a drastic change in the metal−ligand bonding on going from the intermediate to the relevant transition state, making the direct coupling reactions kinetically less favorable.

Acknowledgment. We acknowledge financial support from the Hong Kong Research Grants Council (Grant Nos. HKUST 6023/04P and DAG05/06.SC19) and the University Grants Committee of Hong Kong through the Area of Excellence Scheme (Grant No. Aoe/P-10/01). A.A. appreciates the financial support from Islamic Azad University, Central Tehran Branch, Iran.

Supporting Information Available: Complete ref 17, ONIOM-calculated structures for selected species, and tables giving Cartesian coordinates and electronic energies for all the calculated structures. This material is available free of charge via the Internet at http://pubs.acs.org.

JA063944I